ACCELERATED COMMUNICATION

Kinetic analysis of the binding of monomeric and dimeric ephrins to Eph receptors: Correlation to function in a growth cone collapse assay

KUMAR B. PABBISETTY,[1,5] XIN YUE,[2] CHEN LI,[3] JUHA-PEKKA HIMANEN,[3] RENPING ZHOU,[2] DIMITAR B. NIKOLOV,[3] AND LONGQIN HU[1,4]

[1]Department of Pharmaceutical Chemistry, Ernest Mario School of Pharmacy, Rutgers, The State University of New Jersey, Piscataway, New Jersey 08854, USA
[2]Department of Chemical Biology, Ernest Mario School of Pharmacy, Rutgers, The State University of New Jersey, Piscataway, New Jersey 08854, USA
[3]The Structural Biology Program, Memorial Sloan Kettering Cancer Center, New York, New York 10021, USA
[4]The Cancer Institute of New Jersey, New Brunswick, New Jersey 08901, USA

(RECEIVED October 12, 2006; FINAL REVISION December 8, 2006; ACCEPTED December 16, 2006)

Abstract

Eph receptors and ephrins play important roles in regulating cell migration and positioning during both normal and oncogenic tissue development. Using a surface plasma resonance (SPR) biosensor, we examined the binding kinetics of representative monomeric and dimeric ephrins to their corresponding Eph receptors and correlated the apparent binding affinity with their functional activity in a neuronal growth cone collapse assay. Our results indicate that the Eph receptor binding of dimeric ephrins, formed through fusion with disulfide-linked Fc fragments, is best described using a bivalent analyte model as a two-step process involving an initial monovalent 2:1 binding followed by a second bivalent 2:2 binding. The bivalent binding dramatically decreases the apparent dissociation rate constants with little effect on the initial association rate constants, resulting in a 30- to 6000-fold decrease in apparent equilibrium dissociation constants for the binding of dimeric ephrins to Eph receptors relative to their monomeric counterparts. Interestingly, the change was more prominent in the A-class ephrin/Eph interactions than in the B-class of ephrins to Eph receptors. The increase in apparent binding affinities correlated well with increased activation of Eph receptors and the resulting growth cone collapse. Our kinetic analysis and correlation of binding affinity with function helped us better understand the interactions between ephrins and Eph receptors and should be useful in the design of inhibitors that interfere with the interactions.

Keywords: ephrin; Eph receptor; surface plasmon resonance; receptor dimerization; growth cone collapse

Eph receptor tyrosine kinases (Ephs) are the largest family of receptor tyrosine kinases (Eph Nomenclature Committee 1997). They are classified into two major classes, EphA and EphB, on the basis of their extracellular domain (ECD) sequences and their binding preference to the six glycosylphosphatidylinositol anchor-linked ephrin-A ligands and the three transmembrane ephrin-B ligands (Pasquale 2005). Currently, there are 10 receptors identified from the A class (EphA1-A10) and six receptors from the B class (EphB1-B6) (Himanen and

[5]Present address: Bristol-Myers Squibb Pharmaceutical Research Institute, P.O. Box 4000, Princeton, New Jersey 08543, USA.

Reprint requests to: Longqin Hu, Department of Pharmaceutical Chemistry, Ernest Mario School of Pharmacy, Rutgers, The State University of New Jersey, 160 Frelinghuysen Road, Piscataway, NJ 08854, USA; e-mail: LongHu@rutgers.edu; fax: (732) 445-6312.

Abbreviations: Ephs, Eph receptors; RTK, receptor tyrosine kinase; SPR, surface plasmon resonance; RU, response unit; ECD, extracellular domain; EDC, *N*-ethyl-*N*′-(dimethylaminopropyl)carbodiimide; NHS, *N*-hydroxysuccinimide.

Article and publication are at http://www.proteinscience.org/cgi/doi/10.1110/ps.062608807.

Nikolov 2003; Pasquale 2005). Eph receptors and ephrins are key players in the regulation of cell migration and positioning during both normal development and pathogenesis (Poliakov et al. 2004; Pasquale 2005). They are involved in various biological processes including neural development, cell morphogenesis, tissue patterning, axon guidance, and neural plasticity (Flanagan and Vanderhaeghen 1998; Vogt et al. 1998; Pasquale 2005). Eph receptors are also believed to regulate angiogenesis associated with tumor growth (Dodelet and Pasquale 2000; Ogawa et al. 2000; Brantley et al. 2002), and inhibition of their interactions could lead to the development of a new class of antiangiogenic agents. Blocking of Eph receptor activation using soluble EphA receptors as decoys has been shown to inhibit tumor angiogenesis and progression in vivo in two independent tumor models (the RIP-Tag transgenic model of angiogenesis-dependent pancreatic islet cell carcinoma and the 4T1 model of metastatic mammary adenocarcinoma) (Brantley et al. 2002). In addition, many Eph and ephrin proteins are up-regulated in a wide range of tumors, including melanomas, glioblastomas, and carcinomas of the lung, liver, colon, and breast (Vogt et al. 1998; Tang et al. 1999; Takahashi et al. 2001; Brantley et al. 2002), especially during the more aggressive stages of tumor progression. For example, ephrin-A3 mRNA expression was found to be up-regulated 26-fold in squamous cell lung carcinoma, and EphB2 was expressed ninefold higher in hepatocellular carcinoma compared with healthy liver tissue (Hafner et al. 2004).

Both Eph receptors and ephrins interact predominantly with members of their own class with only a few exceptions, such as EphA4 that binds to ligands from both classes and ephrin-A5 that interacts with EphB2 (Himanen et al. 2004; Pasquale 2005). The current model of Eph–ephrin interaction involves the initial formation of an Eph–ephrin heterodimer complex, which then interacts with another heterodimer complex to form a tetrameric Eph–ephrin complex where each ligand interacts with two receptor monomers and each receptor with two ligand monomers. The tetrameric Eph–ephrin complexes then form higher-ordered Eph–ephrin clusters, which may be responsible for Eph–ephrin signaling (Pasquale 2005). Biological effects attributed to the two membrane-bound proteins are the result of the ''forward'' signaling in Eph-expressing cells and/or the ''reverse'' signaling in the ephrin-expressing cells (Murai and Pasquale 2003). Experimentally, dimerization of an ephrin ligand or Eph receptor is achieved by using the disulfide-linked immunoglobulin Fc-fusion form of the extracellular domain (ECD) of the ligand or receptor. The forced dimeric Fc-fusion proteins can be further cross-linked using anti-Fc IgG antibody to form higher-ordered oligomers. Studies using cross-linked fusion proteins, as well as membrane- or bead-bound proteins, lead to the conclusion that functional Eph/ephrin signaling requires multimerization/aggregation that is facilitated by membrane attachment (Davis et al. 1994; Stein et al. 1998). The kinetic constants of interaction between a dimeric ephrin ligand and a dimeric Eph receptor have been reported for both classes and are in the nanomolar to mid-picomolar range (Lackmann et al. 1997, 1998; Himanen et al. 2004; Day et al. 2005). However, studies reported on monomeric ligands are limited only to the binding of monomeric ephrin-A3 and A5 to EphA3, and the results indicate that monomeric ephrins bind to Eph receptors with much lower affinity (Lackmann et al. 1997; Day et al. 2005). Our interest in designing receptor class-specific antagonists prompted us to determine the binding kinetics of representative ephrin ligand–Eph receptor pairs from both classes and correlate their binding affinities with their biological activities in a functional assay.

Results and Discussion

Surface Plasmon Resonance (SPR) is a sensitive label-free technique that has been widely used to examine the binding kinetics between molecules of biological interest. To use SPR to analyze the interactions of monomeric and dimeric ephrin ligands with their corresponding class of Eph receptors in real time, we needed highly purified ephrin ligands and Eph receptors. For this purpose, we selected ephrin-B2 and EphB2 as the B-class representatives, and ephrin-A5 and EphA3 as the A-class representatives. The extracellular domains of ephrin-B2, EphB2, ephrin-A5, and EphA3 were expressed in stably transfected HEK293 cells as secreted Fc-fusion proteins with a thrombin cleavage site allowing proteolytic Fc-tag removal. Figure 1 illustrates the protein expression and purification of dimeric and monomeric ephrin-A5 as an example. The ephrin-A5-Fc was purified from the

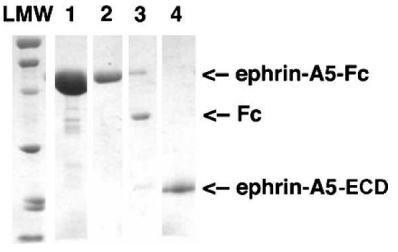

Figure 1. Purification of dimeric and monomeric human ephrin-A5. The protein was expressed as an Fc fusion in HEK293 cells and was purified from culture supernatant by Protein-A Sepharose affinity chromatography (lane *1*) and Superdex-200 size exclusion chromatography (lane *2*). Following thrombin cleavage, the free Fc tag and the uncleaved ephrin-A5-Fc were pulled down using Protein-A beads (lane *3*) to obtain monomeric ephrin-A5 in the supernatant (lane *4*). (LMW) Low Molecular Weight markers—from *top*: 97.4, 66.2, 45.0, 31.0, 21.5, and 14.4 kDa.

HEK293 cell culture supernatant to >90% homogeneity by a single affinity purification step on Protein-A Sepharose. A further size exclusion chromatography step removed most of the remaining contaminating proteins and generated the dimeric ephrin-A5-Fc used in the Biacore and cell-based assays. Monomeric ephrin-A5-ECD was produced after thrombin cleavage of the dimeric Fc tag, and was separated from the uncleaved ephrin-A5-Fc and the Fc fragment with Protein-A Sepharose.

The purified Eph receptor molecules were immobilized onto the carboxymethylated dextran surface of Biacore CM5 sensor chips using the standard amine coupling protocol. Low-density surfaces with ~300–500 response units (RUs) of the receptor proteins were used to minimize mass transfer effects. The SPR sensorgrams for the protein–protein interactions between ephrin and Eph pairs are shown in Figure 2, and the resulting kinetic parameters derived from these sensorgrams are summarized in Table 1.

Analysis of the binding data of ephrin-B2-Fc to EphB2-Fc by the simple first-order rate equation to the Langmuir 1:1 binding model gave an apparent equilibrium dissociation constant of 0.8 nM (Fig. 2A; entry 1, Table 1), which is in agreement with that reported previously (Himanen et al. 2004). Since ephrin-B2-Fc used was in fact a dimer comprised of two ephrin-B2 extracellular domains (ECD) fused with the disulfide-linked immunoglobulin Fc fragments, the SPR sensorgram data were better evaluated with the bivalent analyte model assuming an initial 2:1 interaction, followed by a second 2:2 interaction between ephrin-B2 and EphB2. Such analysis gave an association rate constant of 8.8×10^5 M^{-1} sec^{-1} and a dissociation rate constant of 4.1×10^{-2} sec^{-1}, yielding an equilibrium dissociation constant (K_{D1}) of 4.7×10^{-8} M for the initial 2:1 interaction. This equilibrium dissociation constant of the first ''monovalent'' step matched well with the equilibrium dissociation constant of 2.6×10^{-8} M obtained when the monomeric ephrin-B2-ECD was used instead (Fig. 2B; entry 2, Table 1). In the case of interactions between ephrin-A5 and EphA3, the apparent dissociation constant was 1.3×10^{-12} M for the dimeric Fc-fusion protein, which is within one order of magnitude of the apparent K_D reported recently by Lackmann et al. (Lackmann et al. 1997; Day et al. 2005). Using the bivalent analyte model, the first step of 2:1 binding has an association rate constant of 3.3×10^6 M^{-1} sec^{-1} and a dissociation rate constant of 4.0×10^{-2} sec^{-1}, yielding an equilibrium dissociation constant (K_{D1}) of 1.2×10^{-8} M for the first step (entry 3, Table 1; Fig. 2C). Again, this is comparable to the 8.4×10^{-9} M dissociation constant obtained by using monomeric ephrin-A5-ECD as the analyte (entry 4, Table 1; Fig. 2D). These kinetic results suggest that the decrease in the apparent equilibrium dissociation constants and the increase in the affinity between dimeric ephrins and Eph receptors compared with that between

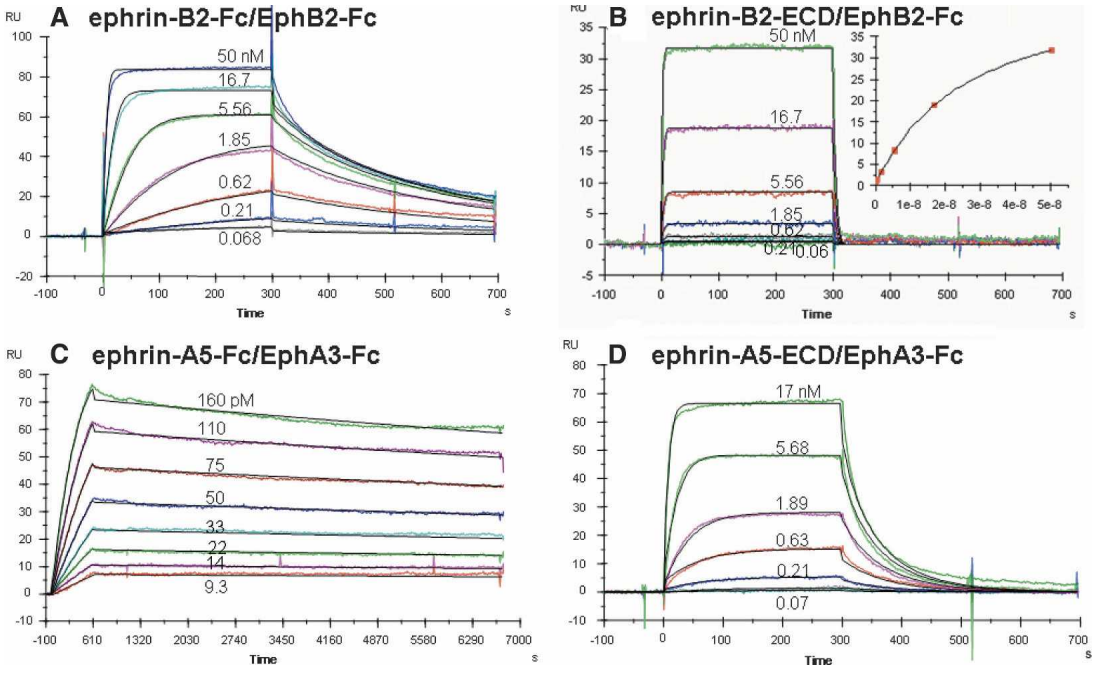

Figure 2. SPR sensorgrams of binding of ephrin-B2 to EphB2 and of ephrin-A5 to EphA3: (*A*) ephrin-B2-Fc interacting with EphB2-Fc, (*B*) ephrin-B2-ECD interacting with EphB2-Fc and the R_{eq} vs. C plot, (*C*) ephrin-A5-Fc interacting with EphA3-Fc, (*D*) ephrin-A5-ECD interacting with EphA3-Fc.

Table 1. *Kinetic parameters for the interaction between ephrin-B2 and EphB2 and that between ephrin-A5 and EphA3 as determined by surface plasmon resonance*

Entry	Ligand	Receptor	1:1 Langmuir binding ($L + R \rightleftarrows LR$)	$\chi^{2\,a}$	Bivalent analyte model ($L_2 + 2R \rightleftarrows L_2R + R \rightleftarrows L_2R_2$)	$\chi^{2\,a}$
1	ephrin-B2-Fc (dimer)	EphB2-Fc (dimer)	$k_a = 6.0 \times 10^6\ M^{-1}\ sec^{-1}$ $k_d = 5.2 \times 10^{-3}\ sec^{-1}$ $K_D = 8.0 \times 10^{-10}\ M$	8.2	$k_{a1} = 8.8 \times 10^5\ M^{-1}\ sec^{-1}$ $k_{d1} = 4.1 \times 10^{-2}\ sec^{-1}$ $K_{D1} = 4.7 \times 10^{-8}\ M$ $k_{a2} = 3.0 \times 10^{-3}\ RU^{-1}\ sec^{-1}$ $k_{d2} = 1.1 \times 10^{-2}\ sec^{-1}$	0.8
2	ephrin-B2-ECD (monomer)	EphB2-Fc (dimer)	$K_D{}^b = 2.6 \times 10^{-8}\ M$	0.1		
3	ephrin-A5-Fc (dimer)	EphA3-Fc (dimer)	$k_a = 2.8 \times 10^7\ M^{-1}\ sec^{-1}$ $k_d = 3.6 \times 10^{-5}\ sec^{-1}$ $K_D = 1.3 \times 10^{-12}\ M$	0.5	$k_{a1} = 3.3 \times 10^6\ M^{-1}\ sec^{-1}$ $k_{d1} = 4.0 \times 10^{-2}\ sec^{-1}$ $K_{D1} = 1.2 \times 10^{-8}\ M$ $k_{a2} = 2.4 \times 10^{-1}\ RU^{-1}\ sec^{-1}$ $k_{d2} = 8.0 \times 10^{-3}\ sec^{-1}$	0.5
4	ephrin-A5-ECD (monomer)	EphA3-Fc (dimer)	$k_a = 3.2 \times 10^6\ M^{-1}\ sec^{-1}$ $k_d = 2.7 \times 10^{-2}\ sec^{-1}$ $K_D = 8.4 \times 10^{-9}\ M$	1.0		

The receptors, EphB2-Fc and EphA3-Fc, were immobilized on the CM5 chip surface and the ligands were used as analyte. Analyte concentrations were 50–0.068 nM for the two ephrin-B2 and EphB2 interaction with an association time of 5 min and a dissociation time of 6 min, 160–9.3 pM for the ephrin-A5-Fc and EphA3 interaction with an association time of 10 min and a dissociation time of 100 min, and 17–0.07 nM for the ephrin-A5-ECD and EphA3 interaction with an association time of 5 min and a dissociation time of 6 min. The sensorgram data were evaluated using BIAevaluation 4.1 software to a 1:1 Langmuir binding model except for the interaction between monomeric ephrin-B2-ECD and EphB2-Fc, where a quick off-rate made it necessary to use the steady-state equation and R_{eq} vs. C plot to obtain the K_D. For the dimeric ligands, the data were also fit to the bivalent analyte model.
[a] Goodness of fit was indicated by χ^2 values. The smaller the χ^2, the better the fit.
[b] K_D was determined from the steady state equation using R_{eq} vs. C plot.
(RU) Response unit.

monomeric ephrins and Eph receptors are simply due to avidity effects—the presence of two independent binding sites in a dimeric ephrin. This is probably how the membrane-bound ephrin ligands and Eph receptors increase their affinity through membrane attachment and how the enhanced binding is mimicked by the forced dimerization via the use of immunoglobulin Fc-fusion proteins and by further aggregation via the addition of anti-Fc IgG antibodies. Of course, the presence of additional interaction surfaces or dimerization-dependent structural rearrangements that facilitate the formation of tetramerization or higher-ordered oligomerization cannot be completely ruled out. It should be noted that the Eph receptor monomers behave similarly in terms of ligand binding kinetics as Eph receptor dimers once immobilized on a sensor chip surface, indicating that the surface immobilization could similarly facilitate the formation of dimers. This justifies our use of R to represent receptor monomers in the bivalent model. The maximum ephrin protein bound to the receptor immobilized onto a chip surface (R_{max}) is a parameter that is dependent on the surface density of receptor immobilized and the molecular weight of the ephrin protein. The R_{max} values obtained were consistent with the molecular weights of the ephrin proteins used and the level of immobilization per chip. For example, the R_{max} values obtained for ephrin-B2-Fc ranged from 62 to 85 RU while those for ephrin-B2-ECD were 42–48 RU.

Our analyses reveal that the increase in binding affinity of the dimeric ephrins for the Eph receptors is due to a dramatic decrease in apparent dissociation rate constant, k_d (e.g., $2.7 \times 10^{-2}\ sec^{-1}$ for ephrin-A5-Fc to EphA3-Fc vs. $3.6 \times 10^{-5}\ sec^{-1}$ for ephrin-A5-ECD to EphA3-Fc), which is consistent with the increased avidity of bivalent 2:2 interactions. Interestingly, comparison of the increase in apparent affinity from monomeric to dimeric ephrin ligands between the A- and B-classes indicates that the forced dimerization using Fc fusion was more effective in the case of the ephrin-A5 ligand, leading to a dramatic 6000- to 9000-fold decrease in apparent dissociation constants, compared with only ~30- to 60-fold decrease in the case of ephrin-B2. Such a dramatic difference in the effects of dimerization on the apparent affinities was unexpected but could be due to the varying structural restrictions placed on the binding domains by the adjacent Fc domains, which may not always allow for optimal protein positioning during the formation of tetrameric ligand–receptor complexes. In the case of the ephrin-A5-Fc/EphA3-Fc interaction, there might be fewer structural restrictions due to Fc fusion, while the second binding event during the ephrin-B2-Fc/EphB2-Fc complex formation might be more affected by Fc fusion, leading to a reduced enhancement in the overall binding affinity. Of course, we cannot yet completely exclude the effect of intrinsic structural differences between the two classes.

To determine the effect of the increased binding affinity on the biological function of ephrins, we further determined their activities in a growth cone collapse assay using dissected rat hippocampi. Rat hippocampi contain both classes of Eph receptors and, therefore, respond to both classes of ephrin ligands. The neuronal projections, or axons, are tipped by growth cones, the growth of which is inhibited when ephrins interact with Eph receptors (Drescher et al. 1995). The primary neuronal culture was selected over other artificial systems because it would make our studies more relevant to the biological functions of ephrins. We compared the effects of different concentrations of monomeric, dimeric, and aggregated (anti-Fc IgG cross-linked) ephrin-B2 and ephrin-A5 on the growth cones in rat hippocampus cultures at different concentrations. Figure 3 shows the percentage of intact growth cones remaining after incubation with various concentrations of the proteins under investigation. Although further studies are needed to characterize which Eph receptor was responsible for the observed activity to a given ligand, the results clearly indicate that growth cone collapse is a function of the multimerization state and concentration of the ephrin ligands and correlates well with the apparent equilibrium dissociation constants. Monomeric ephrins were the least effective in causing growth cone collapse. The monomeric ephrin-B2-ECD did not cause any significant changes in the number of growth cones at all three concentrations used, while 10 nM of the dimeric ephrin-B2-Fc caused a significant decrease in the number of growth cones. Aggregation using anti-Fc IgG antibodies further enhanced the growth cone collapse. Consistent with the increased binding affinity of the ephrin-A5 constructs relative to ephrin-B2, the concentration needed to cause growth cone collapse was lower for the ephrin-A5 than for the corresponding ephrin-B2 constructs. Although it is possible that there are differences in the expression of the two different classes of Eph receptors in the axons, there is a clear correlation between the biological activity and the receptor binding affinity of the different ephrin forms. The results in Figure 3B also document that monomeric ephrin-A5 causes ~50% reduction in growth cones at 100 nM compared with the control. Furthermore, monomeric ephrin-A5 at a concentration of 100 nM was comparable to, if not surpassing, the effect on growth cones caused by dimeric ephrin-A5-Fc at a concentration of 1 nM. This is somewhat unexpected, as the dimeric ephrin-A5 has a 6000-fold lower equilibrium dissociation constant than the monomeric form for binding to its receptor. It is also evident that just occupying the receptor is not sufficient to cause growth cone collapse, whether the ephrin used is a monomer or dimer, and that the concentrations needed to cause growth cone collapse are much higher than the apparent equilibrium dissociation constants.

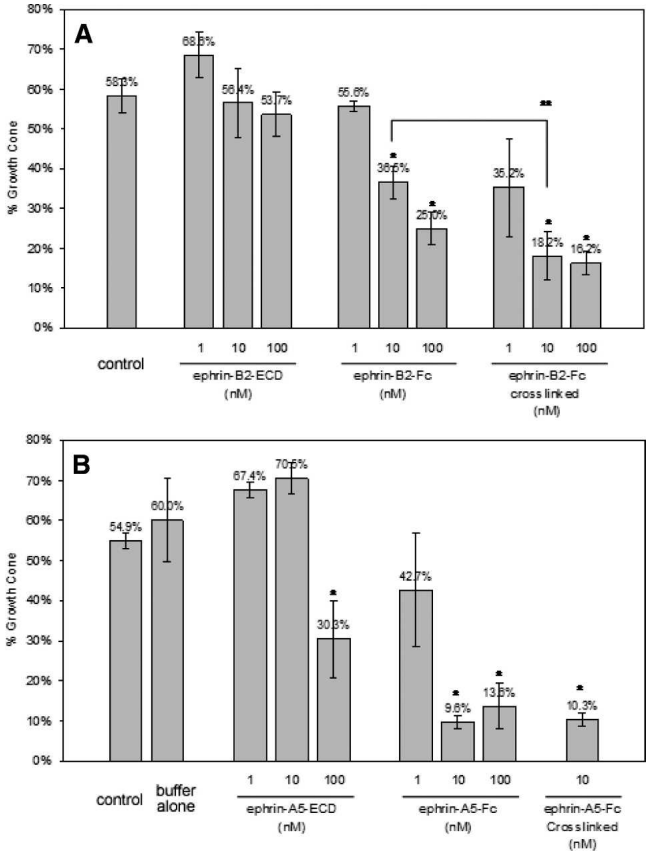

Figure 3. Effect of different forms of ephrin-B2 (*A*) and ephrin-A5 (*B*) on the growth cones from rat hippocampus neurons in a growth cone collapse assay. (*) Statistical significance from the control; (**) statistical significance from ephrin-B2-Fc.

In summary, we evaluated the binding of monomeric and dimeric ephrin-B2 to EphB2 and that of monomeric and dimeric ephrin-A5 to EphA3 using a SPR biosensor and correlated the apparent binding affinities with their functional activities in causing growth cone collapse in neuronal axons. For the first time, we used a bivalent analyte model to analyze the binding kinetics data and demonstrated that the binding of dimeric ephrins to Eph receptors is best described as a two-step process involving a first step of ''monovalent'' 2:1 binding followed by a second step of ''bivalent'' 2:2 binding. Forced dimerization of ephrin ligands through Fc fusion dramatically decreased the apparent dissociation rate constants with little effect on the initial association rate constants, thus effectively decreasing the apparent equilibrium dissociation constants. Our results indicate that dimerization of ephrin-B2 increases the apparent binding affinity between ephrin-B2 and EphB2 by ~30- to 60-fold, while dimerization of ephrin-A5 increases the apparent binding affinity between ephrin-A5 and EphA3 by ~6000-fold. Such a dramatic difference in the effect of dimerization could be

due to varying degrees of structural restrictions caused by the Fc-fusion domains in the different Eph/ephrin complexes. The increase in binding affinities from monomers to dimers and from ephrin-B2 to ephrin-A5 correlated well with enhanced activation of Eph receptors and growth cone collapse. Consistent with the notion that Eph/ephrin signaling requires dimerization or aggregation, monomeric ephrin-B2 did not show any activity in our growth cone collapse assay. However, monomeric ephrin-A5 was unexpectedly found to promote growth cone collapse at high concentrations. These kinetic data and the correlation with biological function provide a better understanding of the interactions between ephrin and Eph receptors, and should facilitate the design of Eph-signaling inhibitors that interfere with the ligand–receptor interactions (Mammen et al. 1998).

Materials and methods

Protein expression and purification

The extracellular regions of murine ephrin-B2 and EphB2, as well as of human ephrin-A5 and EphA3, were expressed as Fc-fusion proteins in HEK293 cells from a modified pcDNA3.1 vector (Invitrogen) containing a CD4 signal sequence (Barton et al. 2005). A thrombin cleavage site followed by a constant domain of IgG was placed at the C terminus of the Eph or ephrin genes. The proteins were purified from cell culture supernatants (DMEM, 10% fetal bovine serum, 20 mg/mL penicillin-streptomycin [Gibco]) by Protein-A Sepharose affinity chromatography (Amersham Biosciences). To obtain monomeric ephrin preparations, the Fc tags were removed by thrombin cleavage and the free Fc tags were pulled down using ProteinA beads. The final step in the purification was size exclusion chromatography on Superdex 200 (Amersham Biosciences), which confirmed that the Fc-fusion ephrins were strictly dimeric, while removal of the Fc tag resulted in strictly monomeric ephrins.

Surface plasmon resonance measurements

Binding of representative ephrin ligands to Eph receptors was carried out on a Biacore 3000 SPR biosensor (Biacore International AB) using EphB2-Fc- and EphA3-Fc-immobilized CM5 chips essentially as described (Lackmann et al. 1997; Day et al. 2005). Briefly, EphB2-Fc and EphA3-Fc (6 μg/mL) were coupled onto CM5 chip surfaces at 10 μL/min using a standard amine coupling protocol with EDC (*N*-ethyl-*N*′-[dimethylaminopropyl]carbodiimide)/NHS (*N*-hydroxysuccinimide). The density was controlled at an increased response level of 300–500 response units (RU), which would yield an R_{max} of ~100 RU in kinetic binding experiments. The ephrin ligand proteins were serially diluted in 10 mM HEPES buffer, pH 7.4 containing 150 mM NaCl, 3.4 mM EDTA, and 0.005% Tween 20 (running buffer), and the kinetic experiments were carried out at 25°C and a flow rate of 50 μL/min unless otherwise noted. The low surface density of sensor chips and the high flow rate were used to minimize mass transport limitation and the effects of steric hindrance. The surface of the sensor chip was regenerated before injecting subsequent samples with 3 M $MgCl_2$ in 0.075 M HEPES buffer containing 25% ethylene glycol, pH 5.8 (the regeneration buffer) at 100 μL/min for 1 min followed by two washes (1 min each) at 100 μL/min with running buffer. All interactions were run with an association time of 5 min and a dissociation time of 6 min except that of ephrin-A5-Fc with EphA3-Fc. Because ephrin-A5-Fc dissociates too slowly from the EphA3-Fc sensor surface, the association phase was extended to 10 min while the dissociation phase was extended to 100 min, both at a flow rate of 25 μL/min. The binding kinetics were analyzed globally using BIAevaluation software 4.1 from the SPR sensorgrams after double subtraction of responses from the reference surface and the zero blank in the absence of ephrin ligands. The single component model of 1:1 Langmuir binding ($L + R \rightleftarrows LR$) was first used for all binding interactions except for that of monomeric ephrin-B2-ECD to EphB2-Fc, where fast dissociation kinetics made it necessary to use the steady state binding (R_{eq}) and the R_{eq} vs. C plot to derive the K_D (BIAapplications Handbook, BIAcore). For the binding of the dimeric ephrin ligands to Eph receptors, the bivalent analyte model ($L_2 + 2R \rightleftarrows L_2R + R \rightleftarrows L_2R_2$) was also used to represent the following interaction between the dimeric ephrin ligands and the immobilized Eph receptors (shown in Scheme 1).

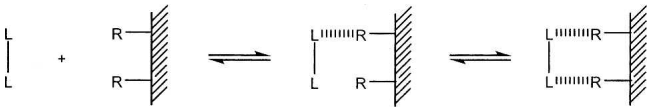

Scheme 1.

Growth cone collapse assay

This assay was performed ex vivo using rat hippocampal explants in essentially the same way as described by Drescher et al. (1995). Briefly, hippocampal explants were isolated from E18 rat embryos and plated onto glass chamber slides coated with poly-D-lysine (0.5 μg/mL, Sigma) and laminin (20 μg/mL, Sigma). Explant cultures were maintained at 37°C in a humidified incubator gassed with 5% CO_2 in Neurobasal medium supplemented with B27 and 2 mM L-glutamine (Invitrogen). After 24 h in culture, various concentrations of monomeric ephrin-ECD and dimeric ephrin-Fc-fusion proteins as well as cross-linked ephrins (10:1 molar ratio for ephrin-Fc and anti-Fc IgG) were added to the explant cultures. After various incubation times (15, 30, or 60 min), the cultures were fixed in 4% paraformaldehyde in phosphate buffered saline for 1 h at room temperature and incubated with Alexa Fluor-Phalloidin (200 U/mL in ethanol) (Molecular Probes, Inc), an orange fluorescent compound that binds to F-actin. Ephrins normally induce growth cone collapse that is concentration-dependent. Criteria for collapsed growth cones are a total loss of filopodia and lamellipodia and a strong decrease in F-actin content. Images were collected with a Sony CCD camera and a PC using ImagePro image analysis software. The collapsed and noncollapsed growth cones were counted in each culture and the data were analyzed with Microsoft Excel and expressed as mean ± SEM. Statistical analysis among the different groups were done by one-way analysis of variance, and in all analyses, differences were considered statistically significant at $P < 0.05$.

Acknowledgments

This work was supported by grants from the National Institutes of Health (CA104956 to L.H., HD23315 to R.Z., GM075886 to

J.-P.H., and NS38486 to D.B.N), and from the National Science Foundation (IBO-0548561 to R.Z.). We also acknowledge an Academic Excellence Award from Rutgers University for the acquisition of the Biacore 3000 used in this study. We thank Dr. Andrew Chow from Biacore for help with the analysis of SPR data.

References

Barton, W.A., Tzvetkova, D., and Nikolov, D.B. 2005. Structure of the angiopoietin-2 receptor binding domain and identification of surfaces involved in Tie2 recognition. *Structure* **13:** 825–832.

Brantley, D.M., Cheng, N., Thompson, E.J., Lin, Q., Brekken, R.A., Thorpe, P.E., Muraoka, R.S., Cerretti, D.P., Pozzi, A., Jackson, D., et al. 2002. Soluble Eph A receptors inhibit tumor angiogenesis and progression in vivo. *Oncogene* **21:** 7011–7026.

Davis, S., Gale, N., Aldrich, T., Maisonpierre, P., Lhotak, V., Pawson, T., Goldfarb, M., and Yancopoulos, G. 1994. Ligands for EPH-related receptor tyrosine kinases that require membrane attachment or clustering for activity. *Science* **266:** 816–819.

Day, B., To, C., Himanen, J.-P., Smith, F.M., Nikolov, D.B., Boyd, A.W., and Lackmann, M. 2005. Three distinct molecular surfaces in ephrin-A5 are essential for a functional interaction with EphA3. *J. Biol. Chem.* **280:** 26526–26532.

Dodelet, V.C. and Pasquale, E.B. 2000. Eph receptors and ephrin ligands: Embryogenesis to tumorigenesis. *Oncogene* **19:** 5614–5619.

Drescher, U., Kremoser, C., Handwerker, C., Loschinger, J., Noda, M., and Bonhoeffer, F. 1995. In vitro guidance of retinal ganglion cell axons by RAGS, a 25 kDa tectal protein related to ligands for Eph receptor tyrosine kinases. *Cell* **82:** 359–370.

Eph Nomenclature Committee. 1997. Unified nomenclature for Eph family receptors and their ligands, the ephrins. *Cell* **90:** 403–404.

Flanagan, J.G. and Vanderhaeghen, P. 1998. The ephrins and Eph receptors in neural development. *Annu. Rev. Neurosci.* **21:** 309–345.

Hafner, C., Schmitz, G., Meyer, S., Bataille, F., Hau, P., Langmann, T., Dietmaier, W., Landthaler, M., and Vogt, T. 2004. Differential gene expression of Eph receptors and ephrins in benign human tissues and cancers. *Clin. Chem.* **50:** 490–499.

Himanen, J.P. and Nikolov, D.B. 2003. Eph signaling: A structural view. *Trends Neurosci.* **26:** 46–51.

Himanen, J.P., Chumley, M.J., Lackmann, M., Li, C., Barton, W.A., Jeffrey, P.D., Vearing, C., Geleick, D., Feldheim, D.A., Boyd, A.W., et al. 2004. Repelling class discrimination: Ephrin-A5 binds to and activates EphB2 receptor signaling. *Nat. Neurosci.* **7:** 501–509.

Lackmann, M., Mann, R.J., Kravets, L., Smith, F.M., Bucci, T.A., Maxwell, K.F., Howlett, G.J., Olsson, J.E., Vanden Bos, T., Cerretti, D.P., et al. 1997. Ligand for EPH-related kinase (LERK) 7 is the preferred high affinity ligand for the HEK receptor. *J. Biol. Chem.* **272:** 16521–16530.

Lackmann, M., Oates, A.C., Dottori, M., Smith, F.M., Do, C., Power, M., Kravets, L., and Boyd, A.W. 1998. Distinct subdomains of the EphA3 receptor mediate ligand binding and receptor dimerization. *J. Biol. Chem.* **273:** 20228–20237.

Mammen, M., Choi, S.K., and Whitesides, G.M. 1998. Polyvalent interactions in biological systems: Implications for design and use of multivalent ligands and inhibitors. *Angew. Chem. Int. Ed. Engl.* **37:** 2755–2794.

Murai, K.K. and Pasquale, E.B. 2003. 'Eph'ective signaling: Forward, reverse and crosstalk. *J. Cell Sci.* **116:** 2823–2832.

Ogawa, K., Pasqualini, R., Lindberg, R.A., Kain, R., Freeman, A.L., and Pasquale, E.B. 2000. The ephrin-A1 ligand and its receptor, EphA2, are expressed during tumor neovascularization. *Oncogene* **19:** 6043–6052.

Pasquale, E.B. 2005. EPH receptor signaling casts a wide net on cell behaviour. *Nat. Rev. Mol. Cell Biol.* **6:** 462–475.

Poliakov, A., Cotrina, M., and Wilkinson, D.G. 2004. Diverse roles of Eph receptors and ephrins in the regulation of cell migration and tissue assembly. *Dev. Cell* **7:** 465–480.

Stein, E., Lane, A.A., Cerretti, D.P., Schoecklmann, H.O., Schroff, A.D., Van Etten, R.L., and Daniel, T.O. 1998. Eph receptors discriminate specific ligand oligomers to determine alternative signaling complexes, attachment, and assembly responses. *Genes & Dev.* **12:** 667–678.

Takahashi, T., Takahashi, K., Gerety, S., Wang, H., Anderson, D.J., and Daniel, T.O. 2001. Temporally compartmentalized expression of ephrin-B2 during renal glomerular development. *J. Am. Soc. Nephrol.* **12:** 2673–2682.

Tang, X.X., Evans, A.E., Zhao, H.Q., Cnaan, A., London, W., Cohn, S.L., Cheung, N.K.V., Brodeur, G.M., and Ikegaki, N. 1999. High level expression of EPHB6, EFNB2 and EFNB3 is associated with low tumor stage and high TrkA expression in human neuroblastoma. *Clin. Cancer Res.* **5:** 1491–1496.

Vogt, T., Stolz, W., Welsh, J., Jung, B., Kerbel, R.S., Kobayashi, H., Landthaler, M., and McClelland, M. 1998. Overexpression of Lerk-5/Eplg5 messenger RNA: A novel marker for increased tumorigenicity and metastatic potential in human malignant melanomas. *Clin. Cancer Res.* **4:** 791–797.